

**Mechanistic Investigations of Alcohol Silylation with
Isothiourea Catalysts**

Journal:	<i>Organic & Biomolecular Chemistry</i>
Manuscript ID	OB-ART-09-2021-001732.R1
Article Type:	Paper
Date Submitted by the Author:	27-Oct-2021
Complete List of Authors:	Redden, Brandon; University of South Carolina, Department of Chemistry and Biochemistry Clark, Robert; University of South Carolina, Department of Chemistry and Biochemistry Gong, Ziyuan; University of South Carolina, Chemistry and Biochemistry Rahman, Md. Mamdudur; University of South Carolina, Chemistry and Biochemistry Peryshkov, Dmitry; University of South Carolina, Department of Chemistry and Biochemistry Wiskur, Sheryl; University of South Carolina, Department of Chemistry and Biochemistry; University of South Carolina,

ARTICLE

Mechanistic Investigations of Alcohol Silylation with Isothiourea Catalysts

Received 00th January 20xx,
Accepted 00th January 20xx

Brandon K. Redden,^a Robert W. Clark,^a Ziyuan Gong,^a Md. Mamdudur Rahman,^a Dmitry V. Peryshkov,^a Sheryl L. Wiskur,^{*a}

DOI: 10.1039/x0xx00000x

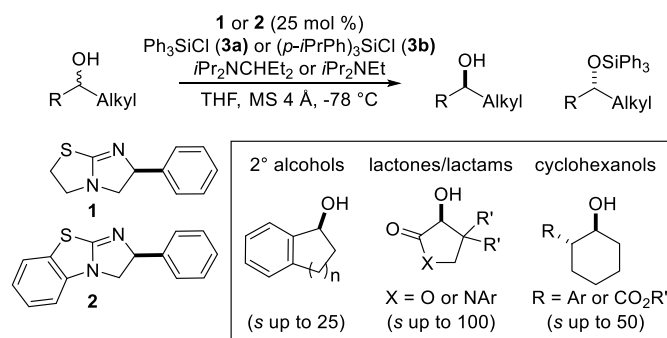
The mechanism of the asymmetric silylation of alcohols with isothiourea catalysts was studied by employing reaction progress kinetic analysis. These reactions were developed by the Wiskur group, and use triphenyl silyl chloride and chiral isothiourea catalysts to silylate the alcohols. While the order of most reaction components was as expected (catalyst, amine base, alcohol), the silyl chloride was determined to be a higher order. This suggested a multistep mechanism between the catalyst and silyl chloride, with the second equivalent of silyl chloride assisting in the formation of the reactive intermediate leading to the rate-determining step. Through the addition of additives and investigating changes in the silyl chloride, an understanding of the catalyst equilibrium emerged for this reaction and provided pathways for further reaction development.

Introduction

Arguably, silyl groups are one of the most common and useful protecting groups in organic chemistry. This protecting group is easy to install and remove, it is orthogonal to other protecting groups, stable to a variety of conditions, and the reactivity of the silyl group is tunable based on the substituents associated with the silicon.¹ More recently, there has been an interest in employing these protecting groups as a means of separating alcohols in kinetic resolutions,² including work done by ourselves.^{3-6,7} With this new wave of research comes the question of how each of these reactions are proceeding mechanistically. Since the 1970's many groups have studied the mechanism of silylation including Corriu,⁸ Bassindale,⁹ and Sommer.¹⁰ This work has essentially led to the conclusion that many different mechanistic pathways are possible depending on the solvent, the leaving group on the silicon, the nucleophilic activator, the substituents on the silicon, etc. This manuscript highlights our efforts to understand the kinetics of our silylation-based kinetic resolution in order to improve our asymmetric silylation methodology. Reaction progress kinetic analysis (RPKA) showed expected orders in alcohol, catalyst, and amine base, but an unexpected higher order in silyl chloride. Herein we investigate the resting state of the catalyst, and how this is affected by changes in catalyst structure, additives, and silyl chloride sterics.

Kinetic resolutions are efficient ways to isolate enantiopure compounds by means of separating a racemic mixture of a compound by selectively reacting with one enantiomer.¹¹ Alcohols have been a very common target for

enantioenrichment via a kinetic resolution, with acylation being the most common mode of derivatization. Recently, there has been an increased interest in employing silyl groups to derivatize one enantiomer over the other. These asymmetric silylation reactions have been performed via dehydrogenative silylation,¹² Bronsted acid catalyzed silylation,¹³ and Lewis base catalyzed silylation.^{3,4,14,15} Specifically, we have developed a silylation-based kinetic resolution that employs the commercially available isothiourea catalysts tetramisole (**1**) and benzotetramisole (**2**),¹⁶ with triphenylsilyl chloride (**3a**) or derivatives (**3b**) to selectively silylate one alcohol enantiomer over another (Scheme 1). We have successfully resolved simple cyclic secondary alcohols,³ alpha hydroxy lactones and lactams,⁴ and 2-aryl and 2-ester cyclohexanols.^{5,6} In order to further improve this methodology, we needed to understand why the reactions proceeded slowly and never fully converted.



Scheme 1. Previous silylation-based kinetic resolutions performed by our group.

While acylation-based resolutions have been well studied, to the best of our knowledge, only a few mechanistic studies of silylation-based resolutions have been published. Hoveyda, Snapper, and coworkers performed a computational study on

^a Department of Chemistry and Biochemistry, University of South Carolina, 631 Sumter St., Columbia, SC 29208, USA. Email: wiskur@mailbox.sc.edu.

Electronic Supplementary Information (ESI) available: See DOI: 10.1039/x0xx00000x

their asymmetric silylation methodology which indicated that two imidazole catalyst molecules could be involved in the mechanism.¹⁵ This aided them in further optimizing their reaction with an achiral co-catalyst, which provided a faster reaction without any loss in selectivity. We ourselves performed a linear free energy relationship study altering the electronics and sterics on the silyl chloride to probe the effect on the reaction.¹⁷ This study indicates that electron donating groups on the silyl chloride slow down the reaction and provide increased selectivity. This allowed us to expand our substrate scope to achieve a higher selectivity with the newly developed silyl chloride derivatized with isopropyl groups (**3b**).⁵ We wanted to further explore the mechanism by discovering the stoichiometry of each reactant and gain some insight into the rate determining step and potential intermediates in the reaction.

Results and discussion

Our mechanistic investigation of isothiurea catalyzed alcohol silylations began with understanding the kinetics via reaction progress kinetic analysis (RPKA). RPKA is an efficient and rapid method for kinetic analysis of a reaction developed by Blackmond.^{18,19,20} This technique allows the investigator to gather kinetic data in fewer experiments than classical approaches,²¹ while providing a complete reaction profile. An additional advantage is the ability to run the reactions under normal experimental conditions, without the large excesses employed in traditional kinetics. Since a kinetic resolution is technically two competing reactions that react at different rates (the rate of the *R* enantiomer reacting versus the *S* enantiomer), exploring the rate of an actual kinetic resolution would be difficult to decipher since both enantiomers would be contributing to the rate. Therefore, the rate studies herein were run with one alcohol enantiomer, (*R*)-tetralol (**4**), which is the fast reacting enantiomer when employing the *S* enantiomers of **1** and **2**.³ Reaction conditions similar to those previously optimized were employed, including triphenylsilyl chloride (**3a**) as the silylating reagent, Hünig's base to neutralize the HCl formed, and THF as the solvent at -78 °C (Eq. 1). Silyl ether (**5**) formation was monitored via in situ IR spectroscopy while confirming conversion via ¹H NMR of aliquots taken at different time points.

The plot of rate versus starting material concentration (Figure 1) immediately reveals interesting information about the reaction. First, it shows that the reaction rate decays very fast early in the reaction, until the alcohol concentration reaches about 40 mM (50% conversion). After that, the reaction rate proceeds very slowly and the reaction has trouble fully converting. Additionally, the plot shows us that the reaction is not first order, given the curve in the data (data is significantly curved away from the dashed linear reference line).²⁰ In order to determine the rate law for the reaction with the order of each component, the "different excess" method of RPKA was used.^{18,20} These experiments reveal the reaction is first order in alcohol **4** and catalyst **1**, zero order in Hünig's base, and interestingly higher order in silyl chloride **3a**. The "different

excess" data for determining the higher order in silyl chloride is shown in Figure 2 (See SI for different excess plots determining order for **4**, **1**, and *i*P₂EtN). The rate of silylation increases with increasing amounts of silyl chloride, but did not overlay when normalized to the concentration of silyl chloride (Figure 2A). This suggests a complex mechanism with a non-integer order in silyl chloride greater than first order kinetics.¹⁹ This higher order is confirmed when the data is normalized by adjusting the exponent of the silyl chloride concentration to 1.5 (Figure 2B), suggesting the reaction is dependent on more than one equivalent of silyl chloride (Table 1, Entry 1).

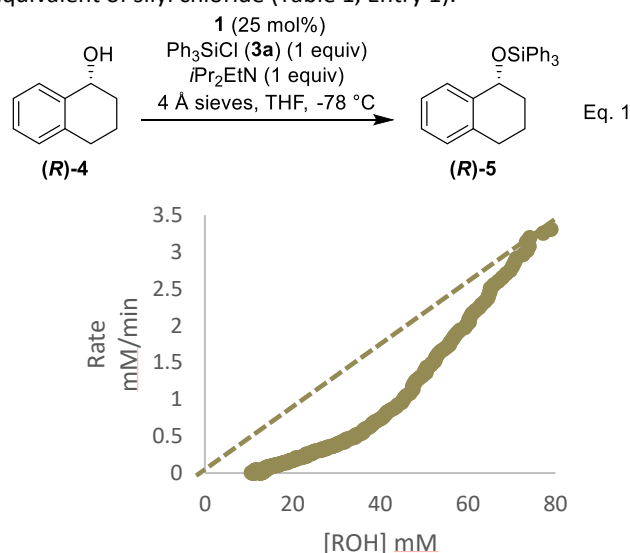


Figure 1. Concentration of alcohol versus rate data collected via in situ IR. Reactions were run at a concentration of 0.08 M with respect to alcohol.

Entry	Catalyst	Silyl chloride	Additive	Order in Silyl Chloride
1	1	Ph ₃ SiCl (3a)	-	1.5
2	2	Ph ₃ SiCl (3a)	-	1.5
3	NMI	Ph ₃ SiCl (3a)	-	0.7
4	1	Ph ₃ SiCl (3a)	NaBARf	0.35
5	1	Ph ₃ SiCl (3a)	Thiourea 5	1.2
6	2	Ph ₂ MeSiCl (3c)	-	1.25
7	2	PhMe ₂ SiCl (3d)	-	1.2

Table 1. The resulting silyl chloride orders upon making changes to the silylation reaction with different catalysts, silyl chlorides, or additives.

Using the "same excess" protocol of RPKA, the reaction can be probed to see if the drop off in rate is indeed due to the decline in silyl chloride concentration, or if something else contributes to the decline in rate, such as catalyst decomposition or product inhibition. Two runs were performed (Table 2) where the silyl chloride was in the same excess with respect to the alcohol at the reaction start. The alcohol concentration was 80 mM (Figure 3, run *a*) and 40 mM (run *b*), while the silyl chloride concentration was 120 mM and 80 mM respectively, giving an "excess" of 40 mM in silyl chloride for both runs. Run *b*, the 40 mM alcohol run, is equivalent to setting up the reaction halfway through the 80 mM alcohol reaction. The runs were compared by adjusting the time of run *b* to the time point where run *a* is

40 mM in alcohol and looking for overlap in the curves. The overlap observed tells us both reactions are behaving the same throughout the reaction, confirming the catalyst is not degrading and the product does not inhibit the reaction. Therefore, the loss in rate can most likely be attributed to the decrease in silyl chloride concentration.

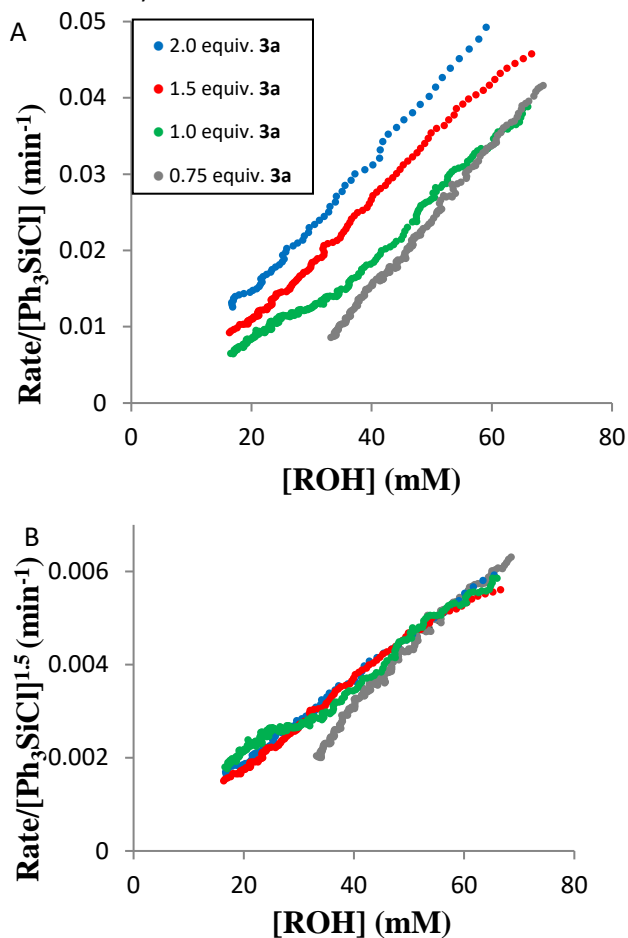


Figure 2. "Different Excess" study to on reaction from Eq. 1 to determine the order of silyl chloride. Reactions were run at a concentration of 0.08 M with respect to **4**, 25 mol% of **1**, the shown equivalents of silyl chloride (0.75-2 equiv) with an equivalent of *i*Pr₂NEt to match the silyl chloride concentration. **A.** The rate normalized to the concentration of silyl chloride. **B.** The rate normalized to the concentration of silyl chloride to the power of 1.5.

Entry	[4]	[3a]	Excess of 3a ¹
1	80 mM	120 mM	40 mM
2	40 mM	80 mM	40 mM

Table 2. Initial reaction conditions carried out at the same excess of **3a** with respect to **4**.

The experimental rate data allowed us to hypothesize the mechanism shown in Scheme 2. The reaction starts with catalyst **1** interacting reversibly with one equivalent of silyl chloride to form intermediate **1** (**Int 1**). The structure of **Int 1** is hypothesized to be the catalyst weakly bonded to the silicon of the silyl chloride in a pentacoordinate manner with the chloride

still attached to the silicon. The literature shows that nitrogen nucleophiles do not outright displace chlorides when reacting with silyl chlorides, even when employing simple combinations that are very reactive, such as trimethylsilyl chloride reacting with *N*-methylimidazole.²² **Int 1** then interacts reversibly with another equivalent of silyl chloride to form intermediate **2** (**Int 2**), which is the reactive intermediate for silylation. We believe the role of the second equivalent of silyl chloride acts as a Lewis acid to aid in removing the chloride from **Int 1**. The alcohol then reacts with **Int 2** in the rate-determining step, transferring the silyl group to the alcohol. The tertiary amine participates after the rate-determining step, and is therefore zero order. With this hypothesized mechanism, we derived a rate equation (Eq. 2). This is a "One-Plus" rate law of the overall silylation reaction where the numerator represents the overall reaction of starting material becoming product, which includes all the rate constants and compounds that affect the rate.²³ The denominator contains three terms that each represent a resting state of the catalyst (free catalyst and the two intermediates). The observed reaction order of 1.5 for the silyl chloride means that the resting state of the catalyst is between free catalyst **1** and **Int 1**, a result of the denominator of Eq. 2 being dominated by $1 + K_{1,eq}[Si]$ and the term $K_{1,eq}K_{2,eq}[Si]^2$ going to zero. This explains why the rate drops so dramatically as the concentration of silyl chloride decreases, further dropping the importance of two of the terms in the denominator.

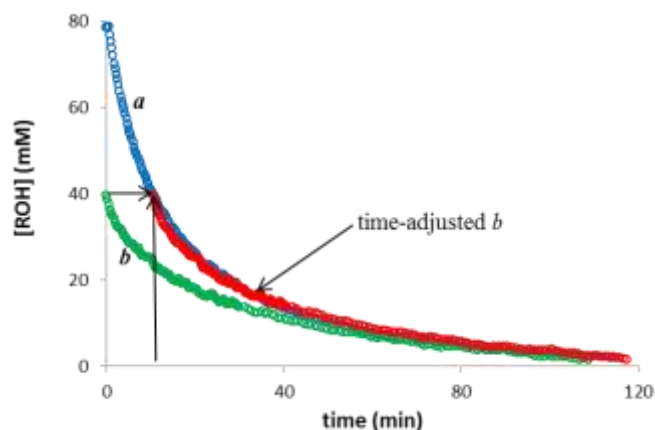
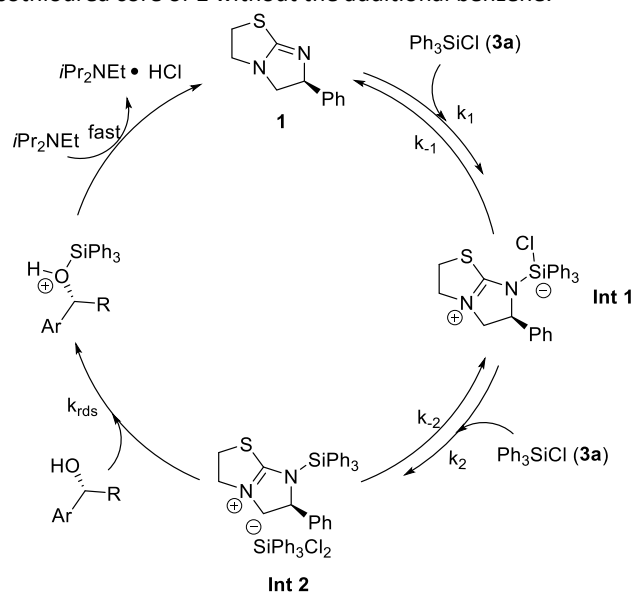


Figure 3. Time-adjusted "Same Excess" experiment. Run *a* started with 80 mM of alcohol; run *b* started with 40 mM of alcohol. Both were run with 20 mM of catalyst and the silyl chloride and *i*Pr₂NEt initial concentrations were 40 mM in excess of the alcohol concentration.

As many of our reactions achieve a greater enantioselectivity using the isothioureia benzotetramisole catalyst **2**, we wanted to investigate if the increased π - π stacking interactions associated with the additional fused aryl ring on the catalyst has any effect on the mechanism and therefore rate law of the reaction. The same experiments were performed using catalyst **2** and the end result was the same, first order in alcohol **4** and catalyst **2**, and a higher order of 1.5 in silyl chloride **3a** (Table 1, Entry 2). The higher order in silyl chloride again shows us that the equilibrium still lies between the free catalyst and **Int 1**. Once more, there was no sign of catalyst degradation or product inhibition in the "same excess" study (See Supporting Info). The

only noticeable difference between the two reactions was that **2** has an initial rate approximately half that of **1**, which is interesting given Mayr's work that shows the isothiourea core of **2** with the fused benzene is more nucleophilic than the isothiourea core of **1** without the additional benzene.²⁴



$$\text{rate} = \frac{k_{rds}K_{1,eq}K_{2,eq}[Si]^2[ROH][cat]_{total}}{1+K_{1,eq}[Si]+K_{2,eq}[Si]^2} \quad \text{Eq. 2}$$

Scheme 2. The proposed mechanism and the "One-Plus" rate law of the overall silylation reaction.

Catalyst	mM/min
1	2.9
2	1.3
NMI	72

Table 3. Initial rate at 10% conversion for the silylation of **4**.

The catalyst that did affect the overall equilibrium of the reaction was *N*-methylimidazole (**NMI**). **NMI** catalyzed the silylation reaction much faster than **1** or **2**, with an initial rate almost 25 times that of **1** (Table 3). Because of the high reaction rate it was difficult finding an equation that provided a good fit to the conversion data, which prevented us from obtaining good rate data. Therefore, a different but similar data analysis method, developed by Burés,²⁵ was used where the time axis is normalized and utilizes the conversion data directly instead of calculating the rate data. The "different excess" experiments showed overlap at a reaction order of 0.7 in silyl chloride (Table 1, Entry 3). When the reaction order falls between zero and one, it shows that the catalyst resting state is between **Int 1** and **Int 2**, and is pushing towards a saturation kinetics model where the rate becomes mostly dependent on the rate-determining step. Mayr's work has shown that isothioureas are more nucleophilic and more Lewis basic than imidazoles,²⁴ yet in this reaction the higher nucleophilicity does not match the equilibrium or rate data. The order of increasing reactivity in

the silylation reaction goes from **2** < **1** < **NMI**, with **NMI** catalyzing the reaction the fastest. This difference in reactivity may be due to the difference in sterics between the catalysts, where **NMI** is relatively unhindered compared to the other two catalysts.

In order to probe the idea that the second silyl chloride drives the formation of **Int 2** via the removal of chloride from **Int 1**, we envisioned employing an additive that would aid in removing the chloride. In theory, this would drive the reaction order of the silyl chloride closer to zero as the dependency on the second equivalent of silyl chloride for the formation of **Int 2** is removed. Two different methods were used to test this. The first method introduced a sodium salt into the reaction, sodium tetrakis [3,5-bis(trifluoromethyl)phenyl]borate (**NaBArF**), which is comprised of a non-coordinating anion that would not affect the reaction mechanism. During the reaction, the sodium pairs with a chloride, forming a highly insoluble salt that precipitates from solution. The removal of chloride drives the formation of **Int 2**, and ultimately causes rapid silylation. An equimolar amount of silyl chloride **3a** and **NaBArF** were employed in a "different excess" study with catalyst **1**, revealing a dramatically increased reaction rate of about 6 times greater than without additive (18 mmol/min versus 3 mmol/min). Again the time axis was normalized to prevent taking a derivative of the rapidly changing conversion data. The analysis showed the silyl chloride reaction order dramatically shifted to 0.35 (Table 1, Entry 4). This indicates a shift toward saturation kinetics where both k_1 and k_2 are large, and k_{rds} dictates the rate of reaction. This means the resting state of the catalyst is between **Int 1** and **Int 2** (Eq. 1). A background reaction was run in the presence of **NaBArF** but no catalyst, resulting in no conversion, showing that **NaBArF** did not have any catalytic effects on the reaction.

The second method to aid in chloride removal was the introduction of a thiourea. Thioureas have strong binding affinities to chloride anions through hydrogen bonds,²⁶ and this attraction was shown by Jacobson to assist some reactions through a substrate chloride abstraction mechanism.²⁷ Again, we envisioned the thiourea to interact with **Int 1** to remove the chloride and shift the equilibrium to **Int 2**. A "different excess" study was conducted, catalyzed by **1**, using the achiral, commercially available *N,N'*-bis[3,5-bis(trifluoromethyl)phenyl]-thiourea (Schreiner's thiourea catalyst, **5**) in equivalent amounts to the catalyst. The initial reaction rate was found to be about four times that of the reaction without the additive (12 mmol/min versus 3 mmol/min). The silyl chloride order was found to be 1.2 using the Blackmond method (Table 1, entry 5), a higher order than what was obtained with **NaBArF**. While the thiourea additive did speed up the reaction and shift the equilibrium a little towards **Int 1** versus without additive, it did not significantly remove the chloride and have as large of an effect as when the sodium precipitated the chloride out of the reaction. This is probably a consequence of the interaction with the chloride being much weaker through hydrogen bonding than the case of removing the chloride from solution altogether

by forming the sodium chloride salt. Additionally, additive **5** was in catalytic amount versus NaBARF being stoichiometric.

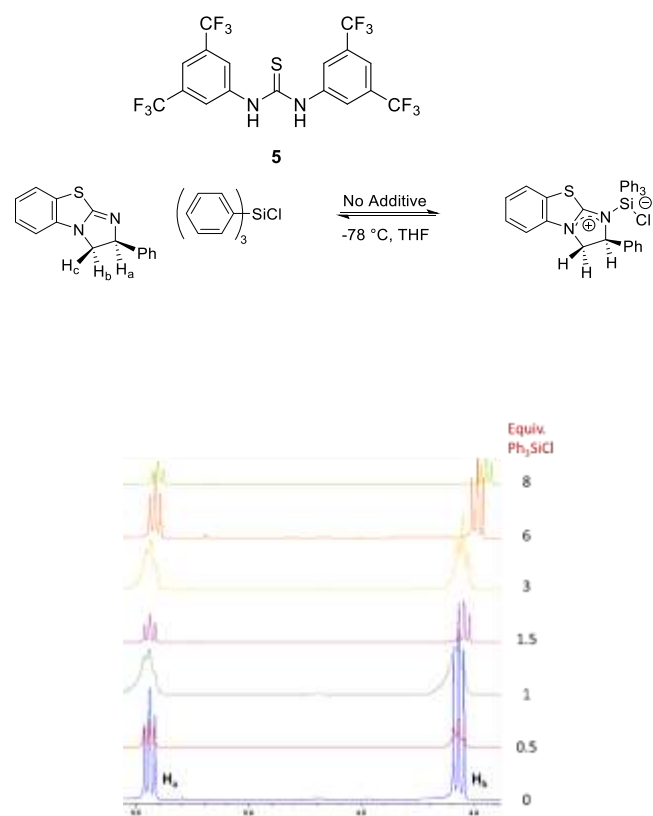


Figure 4. ^1H NMR spectra of **2** (0.16 M in THF) with different amounts of **3a** added. Four drops of benzene- d_6 were added to the THF solutions for locking, and solvent suppression was used to minimize the THF peaks.

A ^1H NMR study was undertaken to further understand the intermediates formed between nucleophilic catalyst **2** and silyl chloride **3a**, both with and without a chloride-sequestering additive. The literature shows that formation of a salt between a nucleophile and a silicon should shift the hydrogens on the nucleophile downfield as they become deshielded.^{22,28} We expected that the alkyl protons ($\text{H}_a/\text{H}_b/\text{H}_c$) on **2** would be sensitive to changes on the nitrogen, and would shift downfield upon complexation with **3a**. Since our reactions are performed in THF, all NMR experiments were done in THF with a small amount of benzene- d_6 for signal lock (THF suppression was performed), and extreme care was taken to exclude water from the experiments. The kinetics suggest that the equilibrium between catalyst **2** and silyl chloride **3a** lies between free catalyst and **Int 1**, and the literature shows that nucleophiles do not displace a chloride from silyl chlorides to form an intermediate salt; therefore, not much was expected upon mixing **2** and **3a**. In the experiments containing only silyl chloride and catalyst, the concentration of **2** was kept constant while the amount of **3a** was increased from 0 to 8 equivalents relative to **2**. This resulted in a very small upfield proton shift (Figure 4), indicating that there is some interaction between the catalyst and silyl chloride, but it is not the result of chloride

displacement. It is likely due to weak electrostatic interactions and suggests, similar to the kinetics, that the catalyst remains mostly in the free state. The data fits a 1:1 binding equation, giving an association constant of 400 M^{-1} confirming a weak interaction between the **2** and **3a**.

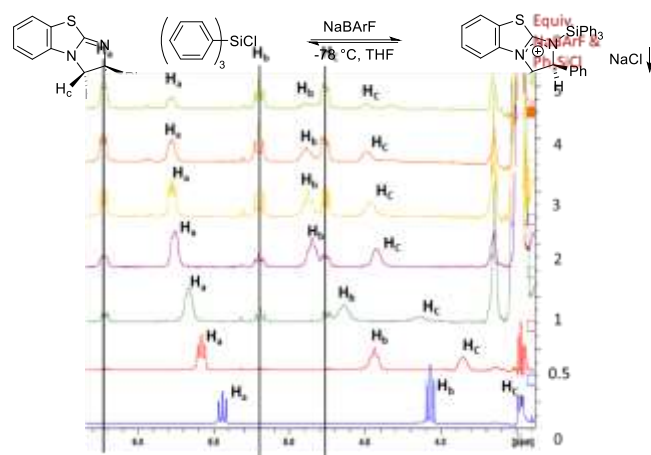


Figure 5. ^1H NMR spectra of **2** (0.09 M in THF) with different equivalents of **3a** and NaBARF present in equivalent ratios to each other. Four drops of benzene- d_6 were added to the THF solutions for locking, and solvent suppression was used to minimize the THF peaks.

Table 4. ^1H NMR ratios of the two peaks formed in Figure 5 upon increasing amounts of NaBARF and **3a**.

Ratios of the Two Species as they Change			
Equiv NaBARF	H_a Ratio	H_b Ratio	H_c Ratio
0.05	3:97	3:97	-
1	15:85	19:81	-
2	24:76	26:74	34:66
3	38:62	39:61	46:54
4	53:47	57:43	59:41
5	68:32	71:29	73:27

The case with NaBARF, however, is much different. The concentration of **2** was again kept constant while equal amounts of **3a** and NaBARF were added from 0 to 5 equivalents relative to **2**. Figure 5 shows an initial downfield shift in all three alkyl proton peaks of **2**. As stated above, a downfield shift of the nucleophile's protons was expected upon complexation with silicon, based on literature precedence. The broadening and shifting of the peaks is an indication of an equilibrium faster than the NMR time scale, presumably between free catalyst and **Int 1**. Interestingly, another species is also present further downfield in the spectra for all three alkyl protons and increases as amount of silyl chloride and NaBARF are increased. We hypothesize this could be the formation of **Int 2** after the removal of the chloride anion, resulting in a further downfield shift. This new peak grows in intensity, indicating that the equilibrium is either slow or non-existent between the new species and the original intermediate formed. A lack of equilibrium would be expected upon removal of chloride from the solution. The area ratio of the two new peaks for each alkyl proton shows a steady increase in the peak furthest downfield and decrease in the other species as more **3a** and NaBARF are

added (Table 4), with similar ratios for each alkyl proton. Due to the solvent suppression of THF, the integration of the peak at 3.5 ppm was difficult to obtain before it shifted further downfield.

To understand how the sterics of silyl chlorides affect the catalyst's resting state, we sequentially removed the large phenyl groups in exchange for methyl groups on **3a** expecting the equilibrium to slowly shift away from free catalyst towards complexed catalyst. This shift would result in a decrease in the order of the silyl chloride. "Different excess" experiments were set up with the slower catalyst **2** using two alternative silyl chlorides, diphenylmethylsilyl chloride (Ph₂MeSiCl, **3c**) and phenyldimethylsilyl chloride (PhMe₂SiCl, **3d**). The smaller silyl chlorides **3c** and **3d** resulted in a dramatic increase in rate versus **3a**, therefore the order in silyl chloride was again determined with the Bures method. With the removal of one phenyl group, the silyl chloride **3c** data normalized to an order of 1.25 (Table 1, entry 6), which is lower than the order of 1.5 for **3a**. The removal of an additional phenyl group had a very similar order of 1.2 for silyl chloride **3d** (Table 1, entry 7), showing that even though the rate increased by exchanging two phenyl groups for methyl groups it did not dramatically shift the catalyst equilibrium. This suggests the resting state of the catalyst is still between free catalyst and **Int 1**, with a slight shift away from free catalyst as a result of the decreased sterics on the silyl chloride.

Experimental

General Information

All kinetic studies were performed with flame-dried glassware under either a nitrogen or argon atmosphere. Molecular sieves were activated in an oven at 170 °C at least 24 h prior to use. Tetrahydrofuran (THF) was degassed and passed through a column of activated alumina prior to use and stored over 4Å molecular sieves. Triphenylsilyl chloride was recrystallized before use. Tetramisole was freebased with NaOH and dried under vacuum prior to use. Sodium tetrakis(3,5-bis(trifluoromethyl)phenyl)borate was recrystallized and dried in a drying pistol before use in both the NMR and kinetic studies, and triphenylsilyl chloride and benzotetramisole were also dried the same way for the NMR binding studies. Unless otherwise stated, all reagents or starting materials were obtained from commercially available sources and used without further purification. The solutions for NMR binding studies and NaBARF kinetic studies were prepared in a glove box. Kinetic experiments were monitored on a Mettler-Toledo ReactIR™ iC10 instrument equipped with a silicon probe. IR data was analyzed using Mettler-Toledo's iC IR software. NMR spectra taken of the kinetic runs were obtained with a 300 MHz Bruker spectrometer and the NMR binding study was done with a 400 MHz Bruker spectrometer. All spectra were obtained in CDCl₃ using TMS as an internal standard (TMS 0.00 ppm for ¹H) unless otherwise stated.

General Procedure for Kinetic Analysis Experiments†

A three-necked reaction vessel was flame-dried, equipped with a flea stir bar and 4Å sieves, and sealed with a septa. The vessel

was purged with nitrogen and the ReactIR probe was inserted into the flask and clamped. A background was taken on air, then the specified amount of THF was added to the reaction vessel and a solvent background was taken. Data recording was initiated, and the solvent was brought to -78 °C using a dry ice/acetone bath. A 1 mL stock solution of dry THF consisting of the alcohol, catalyst, and base was made of which 810 µL was added to the reaction vessel. The reaction was left to equilibrate for 30 minutes. At 30 minutes (t₀), 590 µL of a solution of silyl chloride in THF was added to the reaction flask beginning the reaction. Data was recorded at a rate of one scan every 15 seconds. Aliquots for NMR analysis (~100 µL) were removed and quenched with methanol at various times over the course of the reaction. Aliquots of the reaction were analyzed by ¹H NMR, by integrating the proton peak geminal to the alcohol oxygen for the starting material (tetralol) and the product (silylated derivative). The product proton is observed at 4.96 ppm and the starting material at 4.79 ppm with no overlap from other reaction components. The integrations were used to determine the fraction conversion, which was used to determine the concentration of the remaining alcohol starting material [ROH]. This alcohol concentration was used to determine the Beer's law relationship between absorbance and concentration. After obtaining the Beer's law constants, that information was used to calculate the alcohol concentration from the IR absorbance data by employing the Beer's Law equation.

The percent conversion or product conversation can also be obtained by subtracting the alcohol concentration at each time from the starting alcohol concentration. This data is plotted with time on the x-axis and the percent conversion on the y-axis. The NMR data obtained above was used to confirm both methods give the same conversion data. This ensures the data obtained from the in situ IR is accurate throughout the experiment. With concentration of product [P] obtained at every point of reaction time from in situ IR measurements, the rate of the reaction can now be determined by taking the derivative of an equation that fits the concentration over time data. The conversion versus time data was fit to a 9th-11th order polynomial equation employing a mathematical program (Origin version 6.6 or PolySolve version 3.7). The derivative of this polynomial equation through the use of the power rule yields d[P]/dt, or rate. Prior to the polynomial fit all data was smoothed through simple adjacent three points averaging. This smoothing step facilitates the non-linear curve fitting process. A plot is produced containing rate vs time data. The rate data obtained from this method can then be plotted in various ways to form graphical rate equations.

Conclusions

In conclusion, we investigated the mechanism of silylation of secondary alcohols with triphenylsilyl chloride and the nucleophilic catalysts tetramisole (**1**), benzotetramisole (**2**), and **NMI**. We were able to determine the order of each component, showing that the mechanism employs two equivalents of silyl chloride and two intermediates in the mechanism. Manipulating the sterics on the silyl chloride and driving the

removal of the chloride with salts or thioureas gave us information on the resting state of the catalyst. Further studies will involve exploring the intermediates during silylation and the intermolecular forces that affect selectivity.

Author Contributions

B.K.R., R.W.K., and Z.G kinetic runs and analysis; B.K.R. and M.M.R. NMR studies and analysis. D.V.P supervision of M.M.R. and use of glovebox. S.L.W project and manuscript supervision. All authors have read and agreed to the published version of the manuscript.

Conflicts of interest

There are no conflicts to declare

Acknowledgements

We gratefully acknowledge support from the University of South Carolina and the NSF CAREER Award CHE-1055616 and NSF Award CHE 1856772. We would also like to thank Prof. Donna Blackmond for helpful discussions on this work.

Notes and References

†Details of each run can be found in the supporting information.

- 1 T. W. Greene; P. G. M. Wuts; Third ed.; John Wiley & Sons, Inc.: Hoboken, 1999.
- 2 S. Rendler; M. Oestreich. *Angew. Chem. Int. Ed.* 2008, **47**, 248; A. Weickgenannt; M. Mewald; M. Oestreich. *Org. Biomol. Chem.* 2010, **8**, 1497; L. W. Xu; Y. Chen; Y. Lu. *Angew. Chem. Int. Ed.* 2015, **54**, 9456; J. Seliger; M. Oestreich. *Chem. Eur. J.* 2019, **25**, 9358.
- 3 C. I. Sheppard; J. L. Taylor; S. L. Wiskur. *Org. Lett.* 2011, **13**, 3794.
- 4 R. W. Clark; T. M. Deaton; Y. Zhang; M. I. Moore; S. L. Wiskur. *Org. Lett.* 2013, **15**, 6132.
- 5 L. Wang; R. K. Akhani; S. L. Wiskur. *Org. Lett.* 2015, **17**, 2408.
- 6 T. Zhang; B. K. Redden; S. L. Wiskur. *Eur. J. Org. Chem.* 2019, 4827.
- 7 Z. Papadopulu; M. Oestreich. *Org. Lett.* 2021, **23**, 438.
- 8 R. J. P. Corriu; C. Guerin In *Advances in Organometallic Chemistry*; Stone, F. G. A.; West, R., Eds.; Academic Press: New York, 1982; R. J. P. Corriu; C. Guerin; J. J. E. Moreau In *Topics in Stereochemistry*; Eliel, E. L.; Wilen, S. H.; Allinger, N. L., Eds.; John Wiley & Sons: New York, 1984; Vol. 15.
- 9 A. R. Bassindale; D. J. Parker; P. G. Taylor; R. Turtle. *Z. Anorg. Allg. Chem.* 2009, **635**, 1288.
- 10 L. H. Sommer In *Stereochemistry, Mechanism and Silicon*; McGraw-Hill: New York, 1965.
- 11 H. Kagan; J. Fiaud In *Top. Stereochem.*; Wiley-Interscience New York, 1978; Vol. 10; J. M. Keith; J. F. Larrow; E. N. Jacobsen. *Adv. Synth. Catal.* 2001, **343**, 5; D. Robinson; S. D. Bull. *Tetrahedron: Asymm.* 2003, **14**, 1407; E. Vedejs; M. Jure. *Angew. Chem. Int. Ed.* 2005, **44**, 3974; H. Pellissier. *Adv. Synth. Catal.* 2011, **353**, 1613.
- 12 S. Rendler; G. Auer; M. Oestreich. *Angew. Chem. Int. Ed.* 2005, **44**, 7620; H. F. T. Klare; M. Oestreich. *Angew. Chem. Int. Ed.* 2007, **46**, 9335; S. Rendler; O. Plefka; B. Karatas; G. Auer; R. Fröhlich; C. Mück-Lichtenfeld; S. Grimme; M. Oestreich. *Chem.-Eur. J.* 2008, **14**, 11512; A. Weickgenannt; M. Mewald; T. W. T. Muesmann; M. Oestreich. *Angew. Chem. Int. Ed.* 2010, **49**, 2223; J. Seliger; M. Oestreich. *Angew. Chem. Int. Ed.* 2021, **60**, 247.
- 13 K. Hyodo; S. Gandhi; M. van Gemmeren; B. List. *Synlett* 2015, **26**, 1093; S. Y. Park; J.-W. Lee; C. E. Song. *Nat. Commun.* 2015, **6**, 7512.
- 14 Y. Zhao; J. Rodrigo; A. H. Hoveyda; M. L. Snapper. *Nature* 2006, **443**, 67; Y. Zhao; A. W. Mitra; A. H. Hoveyda; M. L. Snapper. *Angew. Chem. Int. Ed.* 2007, **46**, 8471; T. Isobe; K. Fukuda; Y. Araki; T. Ishikawa. *Chem. Commun.* 2001, 243; Z. You; A. H. Hoveyda; M. L. Snapper. *Angew. Chem. Int. Ed.* 2009, **48**, 547; J. M. Rodrigo; Y. Zhao; A. H. Hoveyda; M. L. Snapper. *Org. Lett.* 2011, **13**, 3778; X. Sun; A. D. Worthy; K. L. Tan. *Angew. Chem. Int. Ed.* 2011, **50**, 8167; A. D. Worthy; X. Sun; K. L. Tan. *J. Am. Chem. Soc.* 2012, **134**, 7321; Z. X. Giustra; K. L. Tan. *Chem. Commun.* 2013, **49**, 4370; X. Sun; H. Lee; S. Lee; K. L. Tan. *Nature Chem.* 2013, **5**, 790; X. Sun; A. D. Worthy; K. L. Tan. *J. Org. Chem.* 2013, **78**, 10494; S. Yoshimatsu; A. Yamada; K. Nakata. *J. Org. Chem.* 2018, **83**, 452; S. Yoshimatsu; K. Nakata. *Adv. Synth. Catal.* 2019, **361**, 4679.
- 15 N. Manville; H. Alite; F. Haeffner; A. H. Hoveyda; M. L. Snapper. *Nature Chem.* 2013, **5**, 768.
- 16 V. B. Birman; X. Li. *Org. Lett.* 2006, **8**, 1351.
- 17 R. K. Akhani; M. I. Moore; J. G. Pribyl; S. L. Wiskur. *J. Org. Chem.* 2014, **79**, 2384.
- 18 D. G. Blackmond. *Angew. Chem. Int. Ed.* 2005, **44**, 4302; N. Zotova; F. Valera; D. G. Blackmond; CRC Press-Taylor & Francis Group, 2009.
- 19 N. Zotova; H. Iwamura; S. P. Mathew; D. G. Blackmond In *Trends in Process Chemistry*; Braish, T.; Gadasamatti, K., Eds.; CRC Press: New York, 2008.
- 20 D. G. Blackmond. *J. Am. Chem. Soc.* 2015, **137**, 10852.
- 21 H. Lineweaver; D. Burk. *J. Am. Chem. Soc.* 1934, **56**, 658; A. Cornish-Bowden *Fundamentals of Enzyme Kinetics*; 4th Edition ed.; Wiley-VCH: Singapore, 2012.
- 22 A. R. Bassindale; T. Stout. *Tetrahedron Lett.* 1985, **26**, 3403.
- 23 F. Helfferich, 2-nd Ed 2004, 40, 53 In *Kinetics of Multistep Reactions*; Green, N. J. B., Ed.; Elsevier: Amsterdam, 2004; Vol. 40.
- 24 B. Maji; C. Joannesse; T. A. Nigst; A. D. Smith; H. Mayr. *J. Org. Chem.* 2011, **76**, 5104.
- 25 J. Burés. *Angew. Chem. Int. Ed.* 2016, **55**, 16084; A. Martínez-Carrión; M. G. Howlett; C. Alamillo-Ferrer; R. W. Adams; J. Burés. *Angew. Chem. Int. Ed.* 2019, **58**, 10189; C. D.-T. Nielsen; J. Burés. *Chem. Sci.* 2019, **10**, 348.
- 26 S. Nishizawa; P. Bfihlmann; M. Iwao; Y. Umezawa. *Tetrahedron Lett.* 1995, **36**, 6483; A.-F. Li; J.-H. Wang; F. Wang; Y.-B. Jiang. *Chem. Soc. Rev.* 2010, **39**, 3729; V. B. Bregović; N. Basarić; K. Mlinaric-Majerskić. *Coord. Chem. Rev.* 2015, **295**, 80; L. Cao; J. Zhao; D. Yang; X.-J. Yang; B. Wu In *Hydrogen Bonded Supramolecular Structures*; Li, Z.-T.; Wu, L.-Z., Eds.; Springer: Berlin, 2015.
- 27 K. Brak; E. N. Jacobsen. *Angew. Chem. Int. Ed.* 2013, **52**, 534
- 28 A. R. Bassindale; T. Stout. *J. Chem. Soc. Perkin Trans. II* 1986, 221.